

Climate change imprinting on stable isotopic compositions of high-elevation meteoric water cloaks past surface elevations of major orogens

Christopher J. Poulsen and M. Louise Jeffery

Department of Geological Sciences, University of Michigan, Ann Arbor, Michigan 48109-1005, USA

ABSTRACT

Stable isotope paleoaltimetry has been widely used to estimate Cenozoic surface elevation of major orogens. The influence of global climate change on stable isotope paleoaltimetry is uncertain, with proposals that warming could cause either overestimates or underestimates of past surface elevations. In this study we increase atmospheric $p\text{CO}_2$ by two and four times in an isotope-tracking atmospheric general circulation model to investigate the effect of global warming on oxygen isotopic compositions of precipitation ($\delta^{18}\text{O}_p$) over the continents. As in other climate models, the response in the GENESIS version 3 model to global warming is an amplification of upper troposphere temperatures through enhanced infrared absorption and a reduction in the surface to upper-level temperature gradient. Due to the temperature dependence of isotopic fractionation, vapor $\delta^{18}\text{O}$ ($\delta^{18}\text{O}_v$) follows suit, leading to a reduction in the surface to upper troposphere $\delta^{18}\text{O}_v$ gradient. In regions of subsidence, including the major orogens and deserts, downward mixing of ^{18}O -enriched vapor from the troposphere to the near surface further reduces the lapse rate of $\delta^{18}\text{O}_v$. As a consequence of these effects, the isotopic composition of precipitation in high-elevation regions, including the Tibetan Plateau, Rocky Mountains, European Alps, and Andean Plateau, increases by 3‰–6‰ relative to that at low elevations. Neglect of this climate effect on high-elevation $\delta^{18}\text{O}_p$ has likely led to underestimates of the surface elevation of Cenozoic orogens.

INTRODUCTION

The isotopic compositions ($\delta^{18}\text{O}$, δD) of precipitation and surface water decrease with elevation (Dansgaard, 1964). This altitude effect is mainly attributed to Rayleigh distillation, the progressive depletion of heavy isotopes (^{18}O and D) from vapor and precipitation, as an air mass moves over an orographic barrier and precipitates rain. However, in regions of strong convection or subsidence, air-mass mixing can cause the altitudinal decrease in $\delta^{18}\text{O}$ and δD to deviate from values expected from Rayleigh distillation (Lee et al., 2007). On average, the oxygen isotopic composition of precipitation decreases with elevation at a rate of 2.8‰ km^{-1} (Poage and Chamberlain, 2001).

The altitude-isotope relationship has been exploited to estimate past surface elevations by employing the isotopic composition of near-surface authigenic minerals as a proxy for ancient meteoric waters. Using empirical isotopic lapse rates, changes in the isotopic composition of these minerals in chronosequences are interpreted to estimate the timing and magnitude of past elevation change. This technique, known as stable isotope paleoaltimetry, has been applied to reconstruct Cenozoic paleoelevation histories of the Andean Plateau, Sierra Nevada of California, Basin and Range, Rocky Mountains, Cascade Mountains, European Alps, Southern Alps of New Zealand, Tibetan Plateau, and Himalayas (Mulch and Chamberlain, 2007). Implicit in this technique is accu-

rate knowledge of the local isotopic lapse rate at the time that the proxy was deposited. In lieu of this information, modern isotopic lapse rates are often employed. Several studies have demonstrated that climate change associated with surface uplift can influence past isotopic lapse rates, complicating or compromising paleoaltimetry estimates (Ehlers and Poulsen, 2009; Galewsky, 2009; Poulsen et al., 2010).

The influence of global climate change on stable isotope paleoaltimetry has received less attention, even though the major orogens have been tectonically active through the Cenozoic, an interval of long-term cooling. Using a model of Rayleigh distillation, Rowley and Garzzone (2007) estimated that due to the reduction in equilibrium isotopic fractionation with temperature, a lifting warm air parcel will undergo less isotopic fractionation than a cold one, yielding a smaller isotopic lapse rate. In contrast, using a simple upslope model of orographic precipitation, Molnar (2010) argued that an increase in saturation vapor pressure and specific humidity in a warmer climate will lead to higher orographic rainfall rates, an increase in isotopic fractionation through rain-out, and larger isotopic lapse rates in orogenic settings. Neither of these models accounts for changes in environmental conditions or large-scale dynamics in a warmer climate. These opposing views lead to the unsatisfactory conclusion that paleoaltimetry estimates of Cenozoic surface uplift could be overestimates or

underestimates due to the influence of global climate change on isotopic lapse rates.

In this contribution we investigate the influence of global climate change, and specifically Cenozoic cooling, on oxygen isotopic compositions of precipitation ($\delta^{18}\text{O}_p$) using an isotope-tracking global climate model. We compare results from preindustrial and warm climate scenarios and demonstrate that, due to enhanced upper troposphere warming, isotopic lapse rates in orogenic settings are reduced in a warmer climate.

MODEL DESCRIPTION AND EXPERIMENTS

Three modern-day experiments were completed with atmospheric $p\text{CO}_2$ levels of 1 \times (280 ppmv), 2 \times (560 ppmv), and 4 \times (1120 ppmv) preindustrial levels. The simulations were completed using the GENESIS version 3.0 earth system model, which consists of an atmospheric general circulation model (AGCM) coupled to multilayer models of vegetation, soil and land ice, and snow (Thompson and Pollard, 1997). Sea-surface temperatures and sea ice are computed using a 50 m slab oceanic layer with diffusive heat fluxes and a dynamic sea-ice model. A land-surface transfer model accounts for the physical effects of vegetation, soil, and soil water. Because the representation of topographic gradients is important for simulating rainfall $\delta^{18}\text{O}$ in these regions, a spectral resolution of T63 (~1.9°) was implemented in the AGCM and land-surface model. The AGCM has 18 vertical levels.

In our version of GENESIS, water isotopic transport and fractionation processes have been added to the atmospheric physics (Mathieu et al., 2002). The $^{18}\text{O}/^{16}\text{O}$ and D/H ratios are predicted in atmospheric vapor, liquid, and ice, and also in soil water reservoirs. Fractionation is modeled as a result of condensation and evaporation in the free atmosphere and from surface waters. Atmospheric ratios are transported using the same Lagrangian transport as for bulk vapor and clouds. The simulation of meteoric and seawater $\delta^{18}\text{O}$ and δD in GENESIS has been shown to compare well with modern global observations (Mathieu et al., 2002; Zhou et al., 2008; Poulsen et al., 2010) and paleoproxies of rainfall $\delta^{18}\text{O}$ (Poulsen et al., 2007). In agreement with observations, GENESIS simulates an altitude effect and low

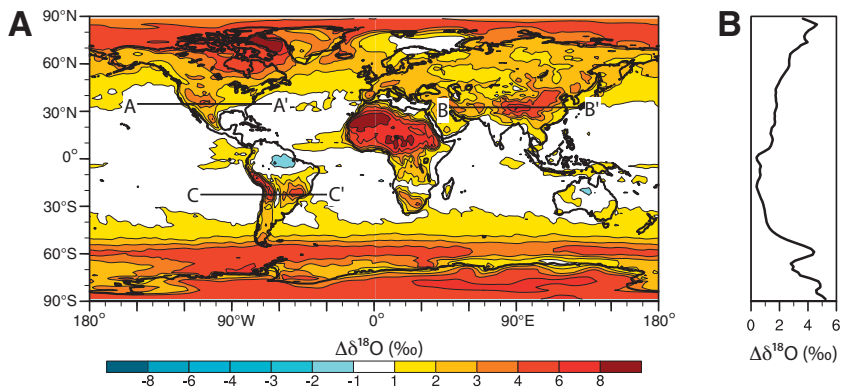
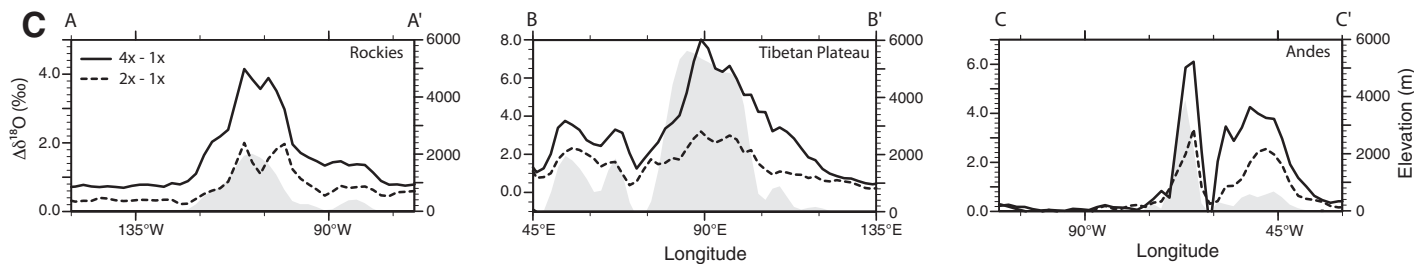


Figure 1. Mean annual amount-weighted surface oxygen isotopic composition of precipitation ($\Delta\delta^{18}\text{O}_p$, ‰) between 4x and 1x experiments. **A:** Global map view of $\Delta\delta^{18}\text{O}_p$. **B:** Zonal-average $\Delta\delta^{18}\text{O}_p$ (‰). Due to reduced isotopic fractionation during surface evaporation, $\delta^{18}\text{O}_p$ increases over most of Earth's surface with 4x increase in $p\text{CO}_2$. Regional changes can deviate substantially from zonal average, particularly in regions of high elevation and subsidence. **C:** $\Delta\delta^{18}\text{O}_p$ (‰) and elevation (m) along longitudinal transects across A-A', North America Rocky Mountains (~35°N); B-B', Tibetan Plateau (~31°N); and C-C', Andean Plateau (~23°S). Dashed line shows $\Delta\delta^{18}\text{O}_p$ between 2x and 1x experiments. Gray shading indicates elevation.



$\delta^{18}\text{O}_v$ (v is vapor) over high-elevation surfaces (Fig. DR1 in the GSA Data Repository¹).

Simulations differ only in the prescription of atmospheric $p\text{CO}_2$. All other boundary conditions, including geography, atmospheric trace gases (CH_4 , N_2O , chlorofluorocarbons), orbital parameters, and land-surface characteristics, were set to A.D. 1991–1995 values. Each simulation was integrated more than 40 model years. The results shown here represent averages over the final 10 model years.

CLIMATE MODEL RESULTS

In GENESIS, the 4x increase in $p\text{CO}_2$ leads to global mean annual warming of 6.5 °C. The primary oxygen isotopic response, $\Delta\delta^{18}\text{O}$, to global warming is an increase in $\delta^{18}\text{O}_p$ due to reduced isotopic fractionation during surface evaporation at higher temperature (Fig. 1). Because of polar amplification of greenhouse warming, high- and mid-latitude regions undergo $\delta^{18}\text{O}_p$ increases of several per mil (‰), while zonal average increases at low latitudes are generally <2‰ (Fig. 1B; Poulsen et al., 2007; Zhou et al., 2008).

Regional $\Delta\delta^{18}\text{O}_p$ varies substantially from the zonal average. In particular, high-elevation regions including the Rocky Mountains, the

Andean Mountains, the European Alps, and the Tibetan Plateau have $\delta^{18}\text{O}_p$ increases of >3‰ and as much as 8‰ (Fig. 1C). The $\delta^{18}\text{O}_p$ increases at high elevations are systematically greater than those at low elevations with the consequence that the $\delta^{18}\text{O}_p$ gradient across orogenic settings decreases by ~2‰–6‰.

The regional changes in surface $\delta^{18}\text{O}_p$ are directly linked to warming in the troposphere. In the 4x experiment, higher temperatures raise the atmospheric saturation vapor pressure according to the Clausius-Clapeyron relation. The increase in saturation vapor pressure enhances surface evaporation and moistening of the atmo-

spheric boundary layer, resulting in higher specific humidity. At low latitudes, where the low-level troposphere is near saturation, convection transports vapor upward, increasing absolute humidity aloft. Moistening enhances troposphere warming through infrared absorption and reduces the surface to upper level temperature gradient (Fig. 2A). The troposphere response to greenhouse gas loading in GENESIS is a robust feature in climate models and has been observed in satellite measurements (Soden et al., 2005).

Due to the temperature (T) dependence of isotopic fractionation, $\Delta\delta^{18}\text{O}_v$ largely mimics ΔT . However, because $\Delta\delta^{18}\text{O}_v$ at any level is a

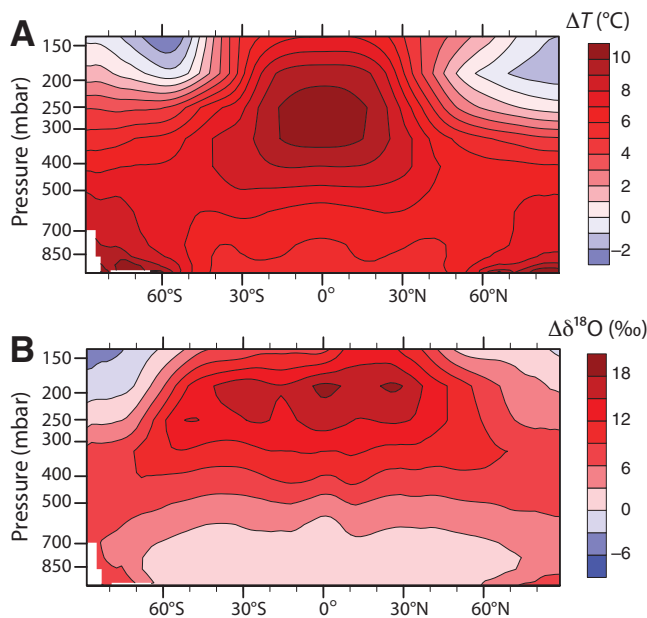


Figure 2. A: Mean annual zonal-average ΔT (temperature) due to global warming through a 4x increase in atmospheric $p\text{CO}_2$. Maximum change in T (°C) occurs in the low-latitude middle to upper troposphere as a result of enhanced latent heating. **B:** Mean annual zonal-average vapor $\delta^{18}\text{O}$ ($\Delta\delta^{18}\text{O}_v$) due to global warming through 4x increase in atmospheric $p\text{CO}_2$. Change in $\delta^{18}\text{O}_v$ (‰) closely follows temperature (see text). In stratosphere (not shown), cooling leads to decrease in $\delta^{18}\text{O}_v$. Unshaded (white) areas represent circumpolar Antarctica.

¹GSA Data Repository item 2011186, supplementary material, Figure DR1 (simulated annual amount-weighted precipitation $\delta^{18}\text{O}_p$ for the modern climate) and Figure DR2 (annual amount-weighted $\delta^{18}\text{O}_p$ predicted using prescribed sea-surface temperatures and a slab-ocean model), is available online at www.geosociety.org/pubs/ft2011.htm, or on request from editing@geosociety.org or Documents Secretary, GSA, P.O. Box 9140, Boulder, CO 80301, USA.

function of the integrated fractionation as the air parcel is lifted from the surface through the troposphere, the maximum tropospheric $\Delta\delta^{18}\text{O}_v$ is offset to higher altitudes relative to the maximum ΔT . The net effect of warming then is to increase troposphere $\delta^{18}\text{O}_v$ and to decrease the near-surface to upper level $\delta^{18}\text{O}_v$ gradient throughout low and middle latitudes (Fig. 2B). In polar regions, surface warming is sufficiently large that increases in surface $\delta^{18}\text{O}_v$ are similar to those in the troposphere, so that the near-surface to upper level $\delta^{18}\text{O}_v$ gradient is not substantially reduced.

The large increase in $\delta^{18}\text{O}_p$ over high-elevation surfaces results from the nonuniform increase in $\delta^{18}\text{O}_v$ through the troposphere. Precipitation forms once an air parcel reaches saturation at the lifting condensation level (LCL). The LCL occurs at higher altitudes over high-elevation surfaces than it does over low-elevation surfaces (note the LCL in Fig. 3). As a consequence, precipitation over high-elevation surfaces condenses from vapor from higher altitudes that is more enriched in ^{18}O due to warming than precipitation that forms over low-elevation surfaces (Fig. 3).

Subsidence of middle and upper troposphere vapor over the orogens further increases high elevation $\delta^{18}\text{O}_p$ in a warmer world. Subsidence in orogenic settings may result through gravity waves, which generate downward motion over a mountain and on its leeward side, in the westward limb of a stationary wave trough, or through large-scale sinking in monsoon regions (Broccoli and Manabe, 1997). Subsidence mixes middle tropospheric vapor, enriched in ^{18}O relative to near-surface vapor, downward over the orogen. This effect can be seen in the downward deflection of $\delta^{18}\text{O}_v$ over the highest elevations (Figs. 3A and 3B) and on the leeward side of the mountains (Figs. 3B and 3C). Rainfall condensed from this vapor is also enriched in ^{18}O . The incursion of ^{18}O -enriched vapor into the lower troposphere is not limited to orogenic regions, but generally occurs in regions of strong subsidence. Saharan low-level $\delta^{18}\text{O}_v$, for example, is 8‰–10‰ higher in the 4× experiment, leading to a $\delta^{18}\text{O}_p$ increase by >6‰ and up to 9‰.

For clarity, we focused here on the isotopic response to a 4× increase in CO_2 . In the 2× experiment, the global average temperature increase is 2.8 °C. The isotopic response in the 2× case is similar but of smaller magnitude than the 4× case (Fig. 1C).

DISCUSSION AND IMPLICATIONS

Modeling Vapor and Precipitation Isotopic Compositions

The isotopic evolution of an air mass undergoing forced ascent is often treated as a Ray-

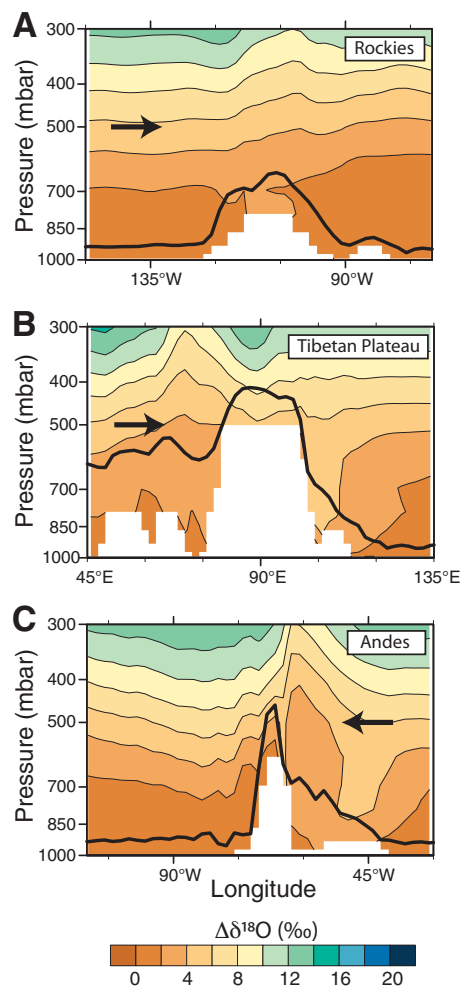


Figure 3. Annual amount-weighted $\delta^{18}\text{O}_v$ (‰), difference in $\delta^{18}\text{O}_v$ between 4× and 1× experiments. **A:** Rocky Mountains (~35°N). **B:** Tibetan Plateau (~31°N). **C:** Andean Plateau (~23°S). Black arrow indicates direction of prevailing winds. Bold black line shows lifting condensation level (LCL), minimum altitude at which air parcel lifted from surface reaches saturation. The $\delta^{18}\text{O}_p$ (p—precipitation) approximately corresponds to $\Delta\delta^{18}\text{O}_v$ at LCL (Fig. DR1; see footnote 1). Unshaded (white) areas represent model topography.

leigh distillation process in which the isotopic composition of the air mass progressively decreases through rainout. This treatment neglects large-scale circulation and mixing between the lifting parcel and its environment. Previous climate modeling and observational studies have shown that mixing during convection and subsidence affects the modern isotopic composition of vapor, causing it to deviate from values expected through Rayleigh distillation. In modern subtropical and monsoonal regions, the intrusion of low δ_v from aloft depletes low-level air in the heavier isotope (Lee et al., 2007; Brown et al., 2008). Similarly, an isotopic rain shadow has been observed on the leeward side

of mountain ranges due to adiabatic cooling and descent of low δ_v air (Blisniuk and Stern, 2005). Our results are consistent with these previous studies, and demonstrate that atmospheric subsidence of vapor enriched in ^{18}O and D in a warmer climate increases high-elevation δ_p and decreases the vertical δ_v gradient.

Some limitations are implicit with the use of a relatively coarse resolution AGCM with a slab-ocean model. Spectral truncation of orography causes smoothing of finer topographic features. Thus, while large-scale isotopic patterns are robust, the model is too coarse to predict detailed patterns of $\delta^{18}\text{O}$ on a mountain range. In addition, the use of a slab-ocean model with zonal sea-surface temperatures may affect the strength and position of deep convection and subsidence. In the modern climate, deep convection occurs primarily over tropical regions of high sea-surface temperature, and is suppressed in tropical regions of oceanic upwelling (Graham and Barnett, 1987). To evaluate the influence of the slab-ocean model on the simulation of $\delta^{18}\text{O}_p$, we compare results from our 1× experiment with a simulation with prescribed modern sea-surface temperatures (Fig. DR2). The use of a slab-ocean model enhances large-scale subsidence over the continents, leading to slightly lower continental $\delta^{18}\text{O}_p$ over subtropical regions and mountains. Because the slab-ocean model was systematically implemented in all experiments, we consider GENESIS predictions of $\Delta\delta^{18}\text{O}$ to be robust. Nonetheless, our results should be viewed as a guide to, but not an absolute prediction of, large-scale $\delta^{18}\text{O}_p$, and require confirmation by higher resolution climate models with dynamic ocean circulation.

Implications for Paleoaltimetry

Our results suggest that stable isotope records in high-elevation regions may be prone to climate overprinting that obscures changes in surface elevations. Is there evidence for this overprinting? Assuming that deep-sea carbonate $\delta^{18}\text{O}$ broadly tracks global climate, the Cenozoic was marked by a warming (~5 °C) through the end Cretaceous and Paleocene, substantial cooling (~7 °C) between the early-middle Eocene and early Oligocene, followed by smaller (~2 °C) cooling events in the late Miocene and Pliocene–Pleistocene (Zachos et al., 2001). Over the same interval, atmospheric CO_2 fell from values generally >1000 ppmv to values <500 ppmv by the early Oligocene, and remained at relatively low levels through the Neogene (Pagani et al., 2005). Two sedimentary $\delta^{18}\text{O}$ records from western North America span this early Cenozoic interval of large climate change. Dettman and Lohmann (2000) reported an ~6‰ increase from the Campanian through the early Eocene in freshwater bivalve shell $\delta^{18}\text{O}$ from the U.S. Western Interior; this

was interpreted to record the isotopic composition of river water that drained the interior basins and adjacent mountains. Horton et al. (2004) reported a $\sim 10\text{‰}$ decrease in middle Eocene to early Oligocene authigenic calcite, smectite, and chert $\delta^{18}\text{O}$ from the Great Basin and Sierra Nevada of North America, and attributed as much as 4‰ of this signal to regional cooling. Although multiple interpretations of these records are possible, we suggest that they track early Cenozoic global warming and cooling trends, providing tentative confirmation of climate overprinting. On the basis of our modeling (Fig. 1A), we estimate that early Cenozoic climate changes could account for as much as $\sim 4\text{‰}$ – 6‰ change in high-elevation sedimentary $\delta^{18}\text{O}$ from western North America, assuming that paleoelevations were similar to modern. If paleoelevations were significantly higher (lower) and consequently influenced by vapor from higher (lower) altitudes, climate change could account for more (less) of the change in sedimentary $\delta^{18}\text{O}$. In other regions, the influence of global cooling on high elevation sedimentary $\delta^{18}\text{O}$ is more difficult to evaluate, mainly because continuous stratigraphic records of early Cenozoic $\delta^{18}\text{O}$ do not exist.

Neglecting the influence of Cenozoic global cooling on $\delta^{18}\text{O}_p$ could lead to substantial underestimates of past surface elevation and overestimates of surface uplift, particularly in the Eocene–Oligocene when cooling was greatest. The isotopic lapse rate in orogenic settings is reduced by $\sim 0.4\text{‰}$ – 1.0‰ km^{-1} and $\sim 1.1\text{‰}$ – 1.5‰ km^{-1} in a warm climate with $2\times$ and $4\times$ preindustrial level $p\text{CO}_2$ (Fig. 1C). Assuming that the global isotopic lapse rate (-2.8‰ km^{-1}) is representative of regional lapse rates, paleoelevation estimates based on proxy estimates of $\Delta\delta^{18}\text{O}$ between high- and low-elevation sites will underestimate the true relief by $>14\%$ and $>40\%$ in climates with $2\times$ and $4\times$ preindustrial level $p\text{CO}_2$. It should be noted that air temperature lapse rates are also affected by global climate change (Fig. 2A). Paleothermometry methods (e.g., Δ_{47}) that rely on reconstructions of temperature lapse rates to infer paleoelevation may also underestimate early Cenozoic surface elevation.

In summary, interpretations of sedimentary $\delta^{18}\text{O}$ from orogenic regions must account for global climate change, in addition to factors such as surface uplift, regional climate change, diagenesis, and fluid contamination. Cenozoic climate change is likely imprinted on high-elevation $\delta^{18}\text{O}$ and δD compositions and has influenced isotopic lapse rates. The magnitude

of overprinting is dependent on the magnitude of troposphere temperature change and the dynamic response over the orogen, influenced by the height of the orogen. Because Cenozoic global climate change is approximately known, it should in principle be possible to estimate this overprinting using isotope-tracking climate models.

ACKNOWLEDGMENTS

This work was supported by the National Science Foundation (grants EAR-0738822, EAR-0907817, EAR-1019420) and the Alexander von Humboldt Foundation. We thank P. Chamberlain, T. Ehlers, N. Insel, and an anonymous reviewer for constructive comments.

REFERENCES CITED

- Blisniuk, P.M., and Stern, L.A., 2005, Stable isotope paleoaltimetry: A critical review: *American Journal of Science*, v. 305, p. 1033–1074, doi:10.2475/ajs.305.10.1033.
- Broccoli, A.J., and Manabe, S., 1997, Mountains and mid-latitude aridity, in Ruddiman, W.F., ed., *Tectonic uplift and climate change*: New York, Plenum Press, p. 89–121.
- Brown, D., Worden, J., and Noone, D., 2008, Comparison of atmospheric hydrology over convective continental regions using water vapor isotope measurements from space: *Journal of Geophysical Research*, v. 113, D15124, doi:10.1029/2007JD009676.
- Dansgaard, W., 1964, Stable isotopes in precipitation: *Tellus*, v. 16, p. 436–468, doi:10.1111/j.2153-3490.1964.tb00181.x.
- Dettman, D.L., and Lohmann, K.C., 2000, Oxygen isotope evidence for high-altitude snow in the Laramide Rocky Mountains of North America during the Late Cretaceous and Paleogene: *Geology*, v. 28, p. 243–246, doi:10.1130/0091-7613(2000)28<243:OIEFHS>2.0.CO;2.
- Ehlers, T., and Poulsen, C.J., 2009, Influence of Andean uplift on climate and paleoaltimetry estimates: *Earth and Planetary Science Letters*, v. 281, p. 238–248, doi:10.1016/j.epsl.2009.02.026.
- Galewsky, J., 2009, Orographic precipitation isotopic ratios in stratified atmospheric flows: Implications for paleoelevation studies: *Geology*, v. 37, p. 791–794, doi:10.1130/G30008A.1.
- Graham, N.E., and Barnett, T.P., 1987, Sea surface temperature, surface wind divergence, and convection over tropical oceans: *Science*, v. 238, p. 657–659, doi:10.1126/science.238.4827.657.
- Horton, T.W., Sjostrom, D.J., Abruzzese, M.J., Poage, M.A., Waldbauer, J.R., Hren, M., Wooden, J., and Chamberlain, C.P., 2004, Spatial and temporal variation of Cenozoic surface elevation in the Great Basin and Sierra Nevada: *American Journal of Science*, v. 304, p. 862–888, doi:10.2475/ajs.304.10.862.
- Lee, J.-E., Fung, I., DePaolo, D.J., and Henning, C.C., 2007, Analysis of the global distribution of water isotopes using the NCAR atmospheric general circulation model: *Journal of Geophysical Research*, v. 112, D16306, doi:10.1029/2006JD007657.

- Mathieu, R.D., Pollard, D., Cole, J.E., White, J.W.C., Webb, R.S., and Thompson, S.L., 2002, Simulation of stable water isotope variations by the GENESIS GCM for modern conditions: *Journal of Geophysical Research*, v. 107, doi:10.1029/2001JD900255.
- Molnar, P., 2010, Deuterium and oxygen isotopes, paleoelevations of the Sierra Nevada, and Cenozoic climate: *Geological Society of America Bulletin*, v. 122, p. 1106–1115, doi:10.1130/B30001.1.
- Mulch, A., and Chamberlain, C.P., 2007, Stable isotope paleoaltimetry in orogenic belts—The silicate record in surface and crustal geological archives: *Reviews in Mineralogy and Geochemistry*, v. 66, p. 89–118, doi:10.2138/rmg.2007.66.4.
- Pagani, M., Zachos, J.C., Freeman, K.H., Tipple, B., and Bohaty, S., 2005, Marked decline in atmospheric carbon dioxide concentrations during the Paleogene: *Science*, v. 309, p. 600–603, doi:10.1126/science.1110063.
- Poage, M., and Chamberlain, C., 2001, Empirical relationships between elevation and the stable isotope composition of precipitation and surface waters: Considerations for studies of paleoelevation change: *American Journal of Science*, v. 301, p. 1–15, doi:10.2475/ajs.301.1.1.
- Poulsen, C.J., Pollard, D., and White, T.S., 2007, General circulation model simulation of the $\delta^{18}\text{O}$ content of continental precipitation in the middle Cretaceous: A model-proxy comparison: *Geology*, v. 35, p. 199–202, doi:10.1130/G23343A.1.
- Poulsen, C.J., Ehlers, T., and Insel, N., 2010, Onset of convective rainfall during gradual Late Miocene rise of the central Andes: *Science*, v. 328, p. 490–493, doi:10.1126/science.1185078.
- Rowley, D.B., and Garzione, C.N., 2007, Stable isotope-based paleoaltimetry: *Annual Review of Earth and Planetary Sciences*, v. 35, p. 463–508, doi:10.1146/annurev.earth.35.031306.140155.
- Soden, B.J., Jackson, D.L., Ramaswamy, V., Schwarzkopf, M.D., and Huang, X., 2005, The radiative signature of upper tropospheric moistening: *Science*, v. 310, p. 841, doi:10.1126/science.1115602.
- Thompson, S.L., and Pollard, D., 1997, Greenland and Antarctic mass balances for present and doubled CO_2 from GENESIS version 2 global climate model: *Journal of Climate*, v. 10, p. 871–900, doi:10.1175/1520-0442(1997)010<0871:GAAMBF>2.0.CO;2.
- Zachos, J., Pagani, M., Sloan, L., Thomas, E., and Billups, K., 2001, Trends, rhythms, and aberrations in global climate 65 Ma to present: *Science*, v. 292, p. 686–693, doi:10.1126/science.1059412.
- Zhou, J., Poulsen, C.J., Pollard, D., and White, T.S., 2008, Simulation of modern and middle Cretaceous marine $\delta^{18}\text{O}$ with an ocean-atmosphere general circulation model: *Paleoceanography*, v. 23, PA3223, doi:10.1029/2008PA001596.

Manuscript received 6 January 2011

Revised manuscript received 10 February 2011

Manuscript accepted 14 February 2011

Printed in USA